

# Homogeneity Realization for Cluster of Heterogeneous Grid-forming Inverters

Muhammad F. Umar, *Student Member, IEEE*, Mohsen Hosseinzadehtaher, *Student Member, IEEE*,  
Mohammad B. Shadmand, *Senior Member, IEEE*

Intelligent Power Electronics at Grid Edge (IPEG) Research Laboratory  
Department of Electrical & Computer Engineering, University of Illinois Chicago  
mumar6@uic.edu, mhosse5@uic.edu, shadmand@uic.edu

**Abstract**— This paper presents a control scheme for enforcing coherency in a cluster of grid-forming inverters with heterogenous characteristics. Increasing penetration of distributive generation (DG) drives the conventional grid towards more complex structure and a new concept with heterogenous characteristics known as power electronics dominated grid (PEDG). Thus, it becomes more challenging to optimize and perform various analysis without an accurate model that mimics the large-scale networks dynamics. The aggregated and reduced-order models that accurately represent the full-scale network enables optimal coordination and computationally efficient stability assessment in real-time. However, the heterogenous characteristics of the inverter based DGs due to the different filter model parameters, inverter ratings and control algorithms poses a challenge to derive an accurate aggregated model. This paper proposes to acquire homogenous dynamic characteristics via coherency enforcement control to aggregate the cluster of grid-forming inverters into single equivalent model that can accurately predicts the dynamic of a PEDG cluster. The coherency in the dynamic response of the grid-forming inverters is realized by autonomously identifying and emulating an equivalent inertia. Various case studies are presented in this paper that validates the proposed enforcing coherency control scheme.

**Keywords**— grid-forming inverter, PEDG, virtual inertia, heterogenous DERs, aggregated model, homogeneous dynamic response

## I. INTRODUCTION

The modern-age power system is shifting from centralized generation to more inverter-based distributed generation (DG). By increasing penetration of DG, the power system is transitioning into a new concept known as power electronics dominated grid (PEDG) [1]. Although the PEDG aids in the integration of the renewable energy resources and brings flexibility in generation. But sparse and distributive nature of PEDG make the power system complex and convoluted network [2-4]. Thus, realization of a dynamic model becomes a challenging task for such system that can be utilized for optimization, coordination, synchronization, and other operational routines. Coherency-based aggregation methods to achieve the reduced-order model of the non-linear synchronous machines is a significant enabling methodology for optimization and economic dispatch of the existing power system [5]. The coherency identification methods can help to find the physical boundaries of network of generation resources whose voltage phase angles and frequency dynamics are in

similar to the disturbances [6, 7]. Moreover, the coherent behaving generators can be clustered to form a single-aggregated model.

In conventional power system the methods to identify and aggregate the large-order systems proven to be effective to preserve the model dynamics. Furthermore, many insightful information can be extracted from these aggregated models after identification of the coherent dynamic response among the generating sources. Existing coherency identification schemes in power systems can be broadly classified in two categories, (i) signal- based, and (ii) model-based schemes. The signal-based schemes leverage the dynamic wide area signals such as synchrophasors to devise the coherency information of the power system. The advantages of signal-based approaches include swift adaption and low dependence on the data from the model [8]. However, the signals from the wide-area monitoring devices are prone to disturbance and infiltration of malicious data [9].

For the typical model-based coherency schemes, the dynamic model of the synchronous generator based on swing equation is manipulated to find the coherent cluster for known set of generation, demand and configuration of the network [10]. The pioneer and extensive work on the model-based coherency identification and model reduction of the power system was performed in 1980s and 1990s [5, 11]. In [12] a model-based scheme is utilized to perform eigenvalue analysis. The accuracy of this scheme is high if precise information of the model and parameters are known. However, practically in many cases it is not possible to access the model information entirely. The slow- coherency algorithm for grouping of the generators based on the DYNRED software is presented in [13] that utilizes the model-based and eigenvector-based principle similar to standard coherency identification techniques. However, the presented analysis is valid for the specific equilibrium point and suffers from modeling imperfections, parametric uncertainties, and heterogenous network like PEDG.

In PEDG the inverter based DGs form large fraction of the power generation mix. Thus, desirably the concepts of the coherency in power systems should be extended and adapted to the inverter-based DGs to develop the accurate reduced-order and aggregated model of the PEDG. There are very limited methods available in literature for coherency identification in DG intensive grids. For instance, the concept of differential

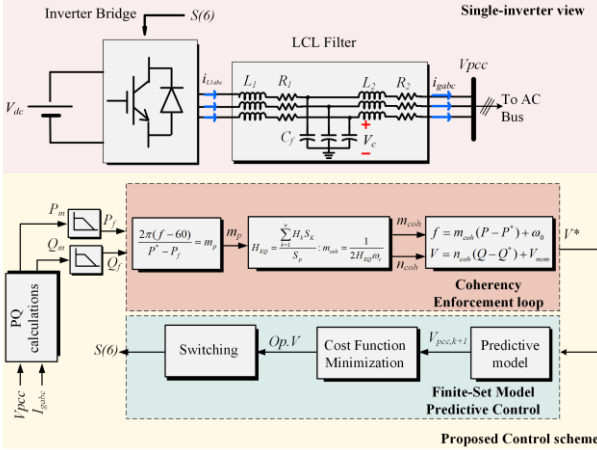


Fig. 1. Proposed system configuration and controller.

geometry to identify the coherent inverters is proposed in [14], but the method applied is complex for large networks and further validation and analysis are required. In [15], coherent equivalence method for modular multilevel inverters (MMI) equipped with virtual synchronous generator (VSG) control is presented. In this scheme the virtual power angles of the VSG-based MMI are exploited to identify the coherent behaving inverters. The developed equivalent model can mimic the dynamic response of the parallel VSG-controlled MMIs with limited accuracy. Nevertheless, a universal and generalized coherency identification scheme for the inverters is still unexplored in the literature. The coherency identification scheme based on the eigenvalue perturbation for droop controlled grid-forming inverter in a feeder is presented in [16]. However, each inverter can have different filter model parameters, controller gain and power ratings. The work in [16] considers all inverter's have similar physical parameters. Therefore, the dynamic response to the disturbance in inverters with dissimilar physical characteristics would not be homogenous and conclusively non-coherent dynamic response.

This paper proposes a coherency enforcement control based on autonomously deriving the equivalent inertia of a grid cluster by inverter's primary layer droop controller gains. The condition for coherency in the grid-forming inverters dictates that if the frequency or voltage angle dynamics after the disturbance such as load increase or decrease is similar for all connected inverters in a cluster then that cluster of inverters can be called coherent. The main contribution of the work is that it considers inverters having different physical characteristic such as filter parameters, control gains and inverter power ratings. This makes the proposed control scheme more realistic as most of the inverters integrated in a modern-day grid are distinct. For instance, these have different manufacturer and depending on that different type of controllers and filter parameters. Therefore, this work encompasses the unexplored domain in the given literature. The rest of the paper is structured as follows: section II presents the formulation of the proposed control. Then, algorithm to enforce the coherency are provided in section III. Simulation results of proposed controller tested under various loading conditions are discussed in section V. Finally, the conclusion of the work is presented in section V.

## II. PROPOSED CONTROL SCHEME ANALYSIS

### A. Coherency enforcement based on virtual inertia emulation

Fig.1 illustrates the control architecture of the proposed control scheme for realization of coherent dynamic response in a cluster of grid-forming inverters. After identifying a grid cluster physical boundaries in PEDG and assuming there are negligible couplings between the voltage and active power and frequency and reactive power, the droop coefficients related to each DG is given as

$$\frac{f - f^*}{P^* - P_f} = \frac{m_p}{2\pi} \quad (1)$$

$$\frac{V - V^*}{Q^* - Q_f} = n_q \quad (2)$$

where,  $f^*$  and  $P^*$  are defined as the nominal frequency and nominal power.  $f$  is the system frequency that is equal to the output frequency of converter.  $P_f$  is the calculated output active power after low-pass filter and  $m_p$  is the droop gain related to active power.  $V^*$  and  $Q^*$  are defined as the nominal voltage and nominal reactive power.  $V$  is the RMS value of the point of common coupling voltage.  $Q_f$  is the calculated reactive power after low-pass filter and  $n_q$  is the droop gain related to reactive power. The calculated power is passed through the low-pass filter to eliminate the low-order variations in the active and reactive power calculations. The mathematical relation of calculated active and reactive power and after passing via low-pass filter is given by,

$$P_f = \frac{P_m}{1 + s/\omega_c} \quad (3)$$

$$Q_f = \frac{Q_m}{1 + s/\omega_c} \quad (4)$$

$\omega_c$  is the cutoff frequency and  $P_m$  and  $Q_m$  is the measured active power and measured reactive power respectively.

The generator swing equation is rearranged to derive the mathematical relationship of emulated virtual inertia from the grid-forming inverter and is given by,

$$\frac{P_m - P^*}{2\pi D_k} = (f - f^*) - \frac{4H\pi f}{D_k} \frac{df}{dt} \quad (5)$$

$$\frac{sf}{\omega_c D_k} + \frac{f - f^*}{D_k} + \frac{P_m - P^*}{2\pi} = \frac{sf}{\omega_c D_k} + \frac{sP^*}{2\pi\omega_c} \quad (6)$$

where  $H$  is defined as the inertia constant and  $D_k$  denotes the damping constant. Investigating equation (5) and (1) reveals that these equations are related by the change in frequency. Specifically, if frequency deviation from the nominal value is small and frequency and power setpoints remain constant, (5) and (1) can be combined and given by (6). Assuming the frequency deviation is small and the right-hand side of (6) is approximately equal to zero. Then relation between inertia constant ( $H$ ) and droop gain ( $m_p$ ) is given as,

$$m_p = \frac{1}{2H\omega_c} ; D_k m_p = 1 \quad (7)$$

The equivalent inertia constant of the entire cluster is calculated, firstly by evaluating the individual inertia constants of the inverters participating in virtual inertia emulation by (7). Then based on the power rating of each inverter's power rating and total power delivered in the cluster. The equivalent inertia is given by,

$$H_{EQ} = \frac{\sum_{k=1}^n H_k S_k}{S_p} = \frac{1}{S_p} \sum_{k=1}^n \frac{S_k}{2m_p k \omega_c} \quad (8)$$

where,  $H_{EQ}$  is the equivalent inertia of the system,  $H_k$  is the individual inertia of the inverter,  $S_k$ ,  $S_p$  are the nominal power of  $k_{th}$  inverters-based DG and the power system under study, respectively, and  $n$  denotes the number of inverters connected in PEDG with emulated virtual inertia. It should be noted that the equivalent inertia is highly dependent on the individual apparent power of the inverter and the rated power of the energy grid.

### B. Predictive control of grid-forming inverter

The controller to regulate the voltage and frequency of the grid-forming inverter is based on model predictive control (MPC). To devise the predictive model[17-19], the state-space representation of the three-phase inverter interfaced with *LCL* filter illustrated in Fig. 1 is given by,

$$\frac{d}{dt} \begin{bmatrix} i_{1,\alpha\beta} \\ v_{c,\alpha\beta} \\ i_{g,\alpha\beta} \end{bmatrix} = A \begin{bmatrix} i_{1,\alpha\beta} \\ v_{c,\alpha\beta} \\ i_{g,\alpha\beta} \end{bmatrix} + B \begin{bmatrix} v_{inv} \\ v_{pcc} \end{bmatrix} \quad (9)$$

where system's A and B matrices are defined as,

$$A = \begin{pmatrix} -\frac{R_1}{L_1} & -\frac{1}{L_1} & 0 \\ \frac{1}{C_f} & 0 & -\frac{1}{C_f} \\ 0 & \frac{1}{L_2} & -\frac{R_2}{L_2} \end{pmatrix} \quad \text{and} \quad B = \begin{pmatrix} \frac{1}{L_1} & 0 \\ 0 & 0 \\ 0 & -\frac{1}{L_2} \end{pmatrix}$$

where  $R_1$ ,  $L_1$ ,  $R_2$ ,  $L_2$ , and  $C_f$  are the discrete values of the passive elements of the output LCL filter,  $i_{1,\alpha\beta}$  is the inverter side current in stationary reference frame,  $i_{g,\alpha\beta}$  is the grid current in stationary reference frame, and  $v_{pcc,\alpha\beta}$  is the point of common coupling voltage stationary reference frame. The discretized version of the state-space model of the inverter presented in (9) is deduced by firstly discretizing the A and B matrices [20, 21],

$$A_d = e^{AT_s}, \quad B_d = \int e^{A\tau} d\tau = \left[ \frac{e^{A\tau}}{A} \right]_0^{T_s} = A^{-1} (A_d - I) B \quad (10)$$

Resultantly, the discretized system matrices in (10) gives the step-ahead prediction for the point of common coupling voltage  $v_{pcc,\alpha\beta,k+1}$ ,

$$\begin{bmatrix} i_{1,\alpha\beta,k+1} \\ v_{c,\alpha\beta,k+1} \\ i_{g,\alpha\beta,k+1} \end{bmatrix} = A_d \begin{bmatrix} i_{1,\alpha\beta,k} \\ v_{c,\alpha\beta,k} \\ i_{g,\alpha\beta,k} \end{bmatrix} + B_d \begin{bmatrix} v_{inv,k} \\ v_{pcc,k} \end{bmatrix} \quad (11)$$

$$v_{pcc,\alpha\beta,k+1} = v_{c,\alpha\beta,k+1} - i_{g,\alpha\beta,k+1} R_2 - L_2 \left( \frac{i_{g,\alpha\beta,k+1} - i_{g,\alpha\beta,k}}{T_s} \right) \quad (12)$$

The voltage reference  $v_{pcc,\alpha\beta,k+1}^*$  for the cost function in (13) are generated by the coherency enforcement controller. This is based on the estimated droop gains  $m_{coh}$  and  $n_{coh}$  that will ensure the coherent behavior of the inverters during the disturbances. The disturbance includes the sudden increase and decrease from the rated value of the load.

Thus, the cost function subject [22] to minimization is given as,

$$g = \left| v_{pcc,\alpha\beta,k}^* - v_{pcc,\alpha\beta,k+1} \right| \quad (13)$$

$$S_{k+1} = \arg \min(g)$$

For each switching vector the cost function is calculated. The switching vectors that minimizes the cost function given in selected as optimized switching vector and then fed to the gates of the inverter [23, 24].

### III. PROPOSED ALGORITHM DESCRIPTION

The proposed control for coherency enforcement is based on devising the specific gains in the reference generation loop. These gains will ensure the coherent behavior of each DG in the identified cluster. Specifically, in the reference generation block of the algorithm, the gains are modified. Moreover, the predictive control for each DG will ensure following the reference generated after incorporating the modified gains. Thus, each DGs with the defined cluster will be forced to behave coherently during the disturbance. Fig. 2 depicts the algorithm for enforcing coherency in the DGs within a cluster. The condition for coherency in the grid-forming inverters dictates that if the frequency dynamics after the disturbance such as load increase or decrease is similar for all connected inverters in a cluster then that cluster of inverters can be called coherent. Firstly, for each DG the inductor  $L_1$  current, capacitor voltage, output current and point of common coupling voltage is measured locally. Then, based on local measurement the per phase active and reactive power is calculated and passed through the low-pass filter. This is necessary to omit any high-frequency ripples on the calculated active and reactive power. Based on the nominal active and reactive power and measured active and reactive power the droop gains are calculated in (1) and (2). To enforce the coherency in DGs within the cluster, the droop gains are modified. This modification is leveraged by calculating the emulated inertia from each DG by (7). After calculating the inertia constant H for each DG, the equivalent inertia constant  $H_{EQ}$  is devised in (8). Thus, based on  $H_{EQ}$  the modified droop gains  $m_{coh}$  and  $n_{coh}$  for each DG are calculated by (8) and that will enforce coherency with the defined cluster. Moreover, the voltage reference based on the modified droop gains is generated for the predictive control loop. In the predictive control the one-step ahead point of common coupling voltage is predicted in (12). Then, cost function is devised in (13) and for each switching vector the cost function is calculated. The switching vector that minimizes the cost function is selected to be optimal switching vector.

TABLE I: SYSTEM SPECIFICATIONS

Parameter	Value
DC Link Voltages $V_{dc}$	600 V
Sampling Time $T_s$	10 $\mu$ s
Inverter-side Inductor $L_1$	5mH
Grid-side Inductor $L_2$	10 $\mu$ H
Filter Capacitance $C_f$	75 $\mu$ F
Inductor Resistance $R_1, R_2$	0.1 $\Omega$
cut-off frequency $\omega_c$	100 rad $s^{-1}$
Inverter rated power $S_1, S_2, S_3$	10 KVAR
Inverter droop gains $m_1, m_2, m_3$	(2.5,3.5,5) $\times 10^{-3} s^{-1}$

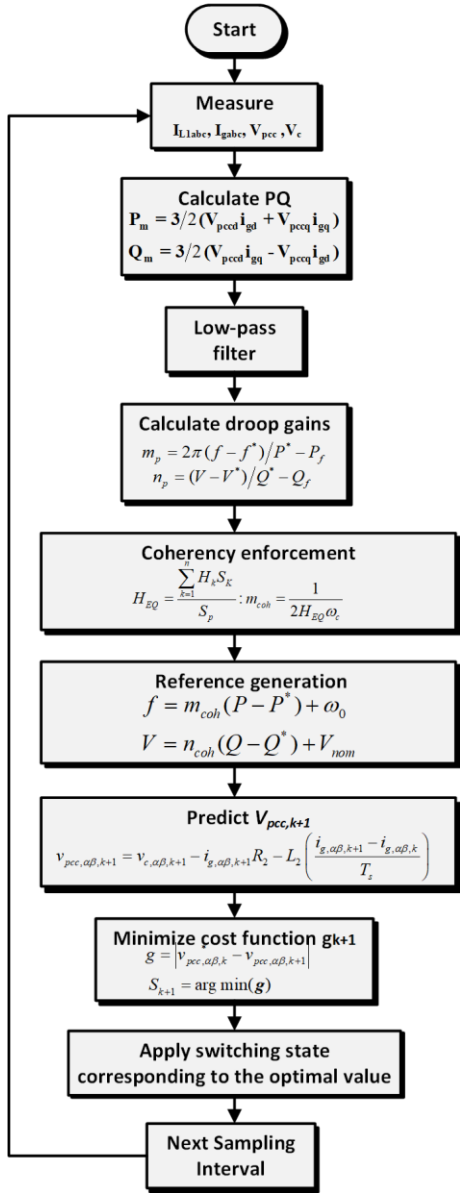


Fig. 2. Algorithm for the proposed control

#### IV. RESULTS AND DISCUSSION

The proposed control scheme is validated for the cluster based on three DGs as illustrated in Fig. 3. The system parameters are specified in the Table I. The functionality of the proposed control scheme is tested under two load disturbances, (i) 50 % load increase on Bus 1, and (ii) 50 % local load reduction. The dynamic frequency response is presented without proposed control, with proposed control and aggregated response.

The case-study A refers to the condition in which the 50% load is increased at instant  $t_1$  on Bus 1 and the impact of this disturbance is studied on the depicted cluster in Fig. 3. Fig. 4(a) shows the frequency dynamic response of the DGs operating independently without the proposed control. At instant  $t_1$ , the

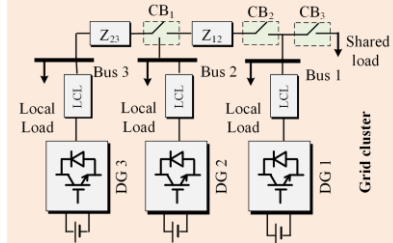


Fig. 3. Configuration of the inverters in the cluster.

load is increased on Bus 1 by 50 %. The frequency dynamic response of each DGs behaves differently and thus, all DGs are non-coherent. However, when same condition is applied after incorporating the proposed control previously non-coherent DGs depicts coherent frequency dynamic response as shown in the Fig. 4(b). The frequency dynamic response shows similar behavior to the disturbance. Moreover, the result with proposed control is compared with aggregated response of the three DGs under the same disturbance. It can be verified by comparing the Fig. 4(b) and (c) that coherent frequency dynamic response achieved by incorporating the proposed control is close to the aggregated response of three DGs. Furthermore, Fig. 4(d) and (e) shows the PCC voltage and output current of DG1 under the load disturbance. At instant  $t_1$ , the output current of DG1 was increased from 20 A<sub>peak</sub> to 30 A<sub>peak</sub> to incorporate the increase in the load. The grid-forming functionality was verified as the voltage remain stiff at 169 V<sub>peak</sub> under this load disturbance.

In the case-study B, a disturbance is injected at instant  $t_2$  by reducing the load to 50 % and the frequency dynamic behavior of three DGs in the cluster is investigated. Fig. 5(a) illustrates the frequency dynamic response of three DGs without the proposed control and it shows the increase in the frequency as the load is reduced. Nevertheless, all DGs have dissimilar frequency transients and concluded to be non-coherent. In Fig. 5(b) the frequency dynamic response of DGs with the proposed control under similar disturbance is shown. In this all the DGs have homogenous frequency transients and concluded to be coherent. Moreover, as compared to the aggregated response of the three DGs in Fig. 5(c) the frequency transients with proposed control are similar. This verifies that under various disturbances the proposed control enforces the coherency in the cluster of the grid-forming inverters. Furthermore, the grid-forming capability is verified in Fig. 5 (d) and (e). As the load was decreased by 50 % the output current of the DG<sub>2</sub> was reduced from 20 A<sub>peak</sub> to 10 A<sub>peak</sub>. However, the

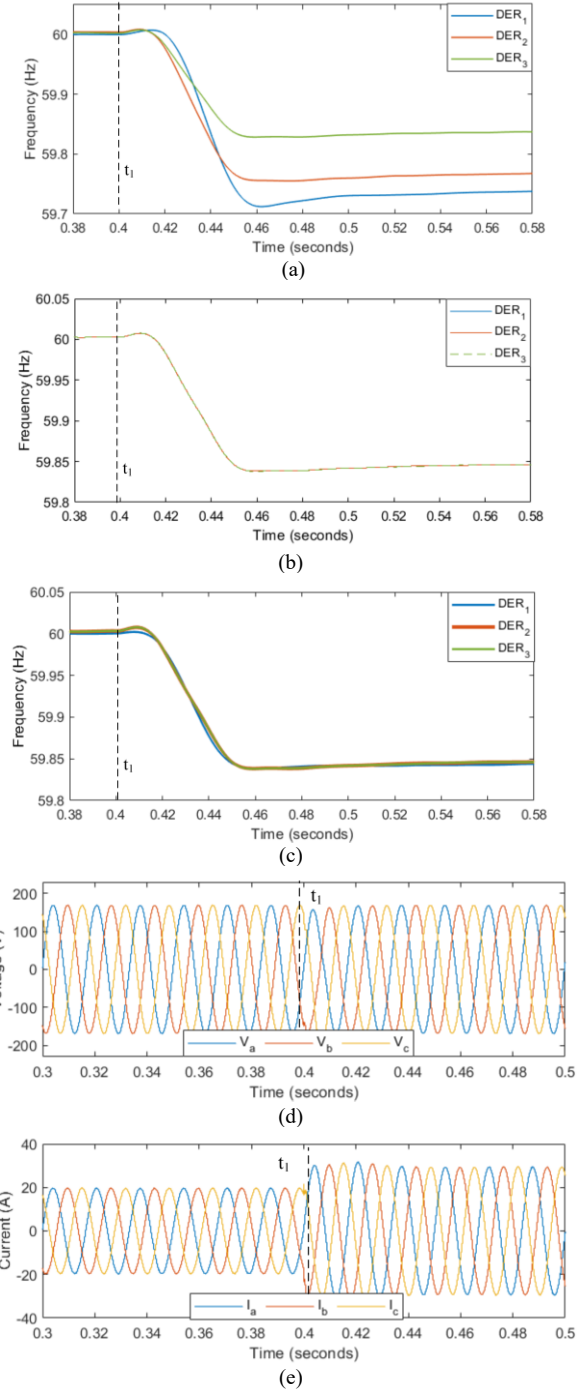


Fig. 4. Case-study A: Frequency dynamic response of the cluster based on grid forming inverters under 50 % load increase on Bus 1: (a) without proposed control, (b) with proposed coherency enforcement control, (c) aggregated response, (d) DG<sub>1</sub> PCC voltage, and (e) DG<sub>1</sub> output current

PCC voltage of the DG2 remains stiff at 169 V<sub>peak</sub>. Thus, this validates the grid-forming ability of the proposed control in both type of load disturbances.

## V. CONCLUSION

This paper presented a control scheme for enforcing coherency in a cluster of grid-forming inverters with heterogenous characteristics. Increasing penetration of distributive

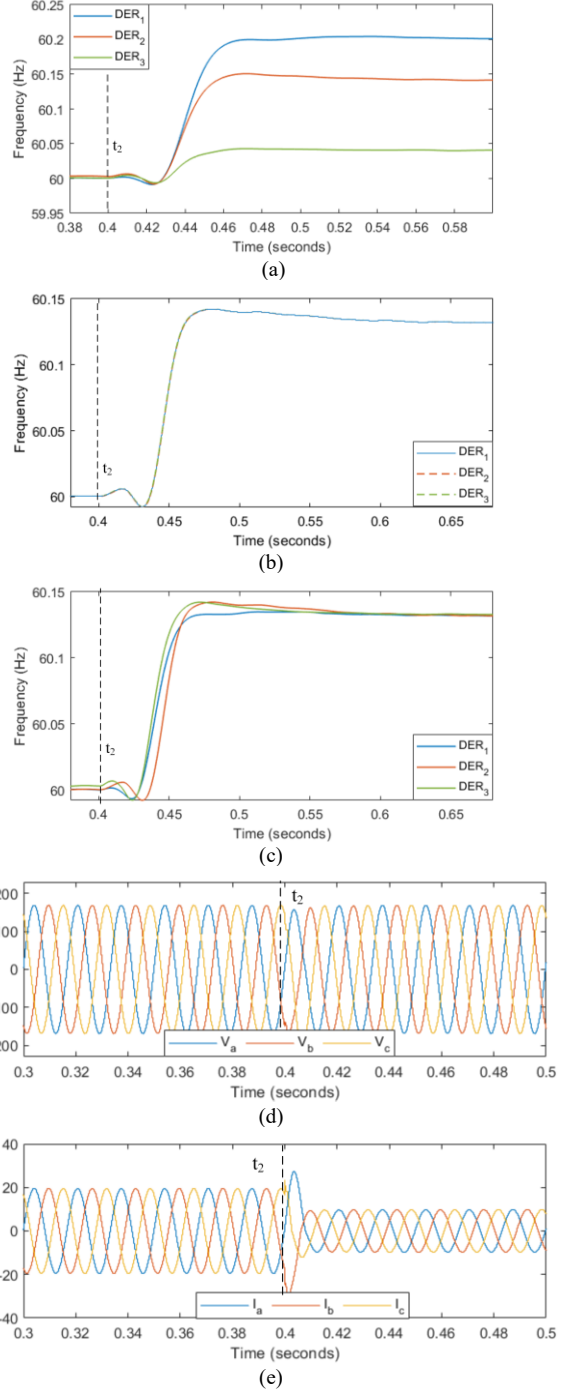


Fig. 5. Case-study B: Frequency dynamic response of the cluster based on grid forming inverters under 50 % load decrease: (a) without proposed control, (b) with proposed coherency enforcement control, (c) aggregated response, (d) DG<sub>2</sub> PCC voltage, and (e) DG<sub>2</sub> output current

generation (DG) drives the conventional grid towards more complex and denser structure. Thus, it become more computationally challenging to optimize and perform various analysis on large-scale networks. The aggregated and reduced-order models that accurately represent the full-scale network can decrease the computational burden significantly. However, the dissimilar characteristics of the inverter based DGs due to the different filter model parameters, inverter ratings and

control algorithms poses a challenge to derive the aggregated model. In various case studies presented in the paper it was concluded with proposed control the non-coherent cluster of inverters can be coherent under various disturbances that includes load increase or load decrease.

#### ACKNOWLEDGMENT

This work was supported by the U.S. National Science Foundation under Grant ECCS-2114442. The statements made herein are solely the responsibility of the author.

#### REFERENCES

- [1] A. Khan, M. Hosseinzadehtaher, M. B. Shadmand, S. Bayhan, and H. Abu-Rub, "On the Stability of the Power Electronics-Dominated Grid: A New Energy Paradigm," *IEEE Industrial Electronics Magazine*, vol. 14, no. 4, pp. 65-78, 2020, doi: 10.1109/MIE.2020.3002523.
- [2] O. H. Abu-Rub, A. Y. Fard, M. F. Umar, M. Hosseinzadehtaher, and M. B. Shadmands, "Towards Intelligent Power Electronics-Dominated Grid via Machine Learning Techniques," *IEEE Power Electronics Magazine*, vol. 8, no. 1, pp. 28-38, 2021.
- [3] Y. Gu, N. Bottrell, and T. C. Green, "Reduced-order models for representing converters in power system studies," *IEEE Transactions on Power Electronics*, vol. 33, no. 4, pp. 3644-3654, 2017.
- [4] M. S. Ali, M. K. Ahmad, M. F. Umar, and S. M. R. Kazmi, "Comparison of non-isolated converter topologies for maximization of energy yield of photovoltaic energy conversion system," in *2018 1st International Conference on Power, Energy and Smart Grid (ICPESG)*, 2018: IEEE, pp. 1-6.
- [5] J. H. Chow, R. Galarza, P. Accari, and W. W. Price, "Inertial and slow coherency aggregation algorithms for power system dynamic model reduction," *IEEE Transactions on Power Systems*, vol. 10, no. 2, pp. 680-685, 1995.
- [6] R. Podmore, "Identification of coherent generators for dynamic equivalents," *IEEE Transactions on Power Apparatus and Systems*, no. 4, pp. 1344-1354, 1978.
- [7] X. Wang, V. Vittal, and G. T. Heydt, "Tracing generator coherency indices using the continuation method: A novel approach," *IEEE Transactions on Power Systems*, vol. 20, no. 3, pp. 1510-1518, 2005.
- [8] V. Terzija *et al.*, "Wide-area monitoring, protection, and control of future electric power networks," *Proceedings of the IEEE*, vol. 99, no. 1, pp. 80-93, 2010.
- [9] N. Senroy, "Generator coherency using the Hilbert–Huang transform," *IEEE Transactions on Power Systems*, vol. 23, no. 4, pp. 1701-1708, 2008.
- [10] G. Rogers, *Power system oscillations*. Springer Science & Business Media, 2012.
- [11] J. H. Chow, *Time-scale modeling of dynamic networks with applications to power systems*. Springer, 1982.
- [12] S. Yusof, G. Rogers, and R. Alden, "Slow coherency based network partitioning including load buses," *IEEE Transactions on Power Systems*, vol. 8, no. 3, pp. 1375-1382, 1993.
- [13] I. Tyuryukanov, M. Popov, M. A. van der Meijden, and V. Terzija, "Slow Coherency Identification and Power System Dynamic Model Reduction by Using Orthogonal Structure of Electromechanical Eigenvectors," *IEEE Transactions on Power Systems*, vol. 36, no. 2, pp. 1482-1492, 2020.
- [14] X. Du, Y. Zhang, Q. Li, Y. Xiong, X. Yu, and X. Zhang, "New theory of extended coherency for power system based on method of coherency in differential geometry," in *2011 Asia-Pacific Power and Energy Engineering Conference, 2011*: IEEE, pp. 1-6.
- [15] C. Li, J. Xu, and C. Zhao, "A coherency-based equivalence method for MMC inverters using virtual synchronous generator control," *IEEE Transactions on Power Delivery*, vol. 31, no. 3, pp. 1369-1378, 2015.
- [16] P. J. Hart, R. H. Lasseter, and T. M. Jahns, "Coherency identification and aggregation in grid-forming droop-controlled inverter networks," *IEEE Transactions on Industry Applications*, vol. 55, no. 3, pp. 2219-2231, 2019.
- [17] M. F. Umar *et al.*, "Single-Phase Grid-Interactive Inverter with Resonance Suppression based on Adaptive Predictive Control in Weak Grid Condition," *IEEE Journal of Emerging and Selected Topics in Industrial Electronics*, 2021.
- [18] M. F. Umar, A. Khan, M. Easley, S. D'Silva, B. Nun, and M. B. Shadmand, "Resonance Suppression based on Predictive Control of Grid-following Inverters with LCL Filter in Weak Grid Condition," in *2020 IEEE Energy Conversion Congress and Exposition (ECCE)*, 2020: IEEE, pp. 4742-4748.
- [19] A. Y. Fard and M. B. Shadmand, "Multitimescale three-tiered voltage control framework for dispersed smart inverters at the grid edge," *IEEE Transactions on Industry Applications*, vol. 57, no. 1, pp. 824-834, 2020.
- [20] B. Nun, M. F. Umar, A. Karaki, M. B. Shadmand, S. Bayhan, and H. Abu-Rub, "Model Predictive Control for Black Start of Connected Communities via Autonomous Indexing," in *2021 IEEE 12th International Symposium on Power Electronics for Distributed Generation Systems (PEDG)*, 2021: IEEE, pp. 1-7.
- [21] B. Nun, M. F. Umar, and M. B. Shadmand, "Enabling Resilient Community Microgrids with Multiple Points of Common Coupling via a Rank-Based Model Predictive Control Framework," in *2021 IEEE Applied Power Electronics Conference and Exposition (APEC)*, 2021: IEEE, pp. 2686-2691.
- [22] M. F. Umar, A. Khan, and M. B. Shadmand, "A stabilizer based predictive control scheme for smart inverters in weak grid," in *2020 IEEE Texas Power and Energy Conference (TPEC)*, 2020: IEEE, pp. 1-6.
- [23] B. Nun, M. F. Umar, A. Karaki, M. B. Shadmand, S. Bayhan, and H. Abu-Rub, "Rank-based Predictive Control for Community Microgrids with Dynamic Topology and Multiple Points of Common Coupling," *IEEE Journal of Emerging and Selected Topics in Industrial Electronics*, 2021.
- [24] M. N. Akbar, M. F. Umar, A. Ulasyar, H. S. Zad, A. Khattak, and S. M. R. Kazmi, "Low Cost Design of a Motor Characterization Test Bed for Control System Validation," in *2019 International Conference on Electrical, Communication, and Computer Engineering (ICECCE)*, 2019: IEEE, pp. 1-6.